Study of Self-Generated Magnetic Fields by Femtosecond Laser Plasma Interactions

A. Abudurexiti (阿不都热苏力), T. Tuniyazi (帕尔哈提)

(*Department of Physics, Xinjiang University, Urumqi, Xinjiang* 830046, *China*)

* *Corresponding author*: *abdrusul@sina.com*

Received May 20,2012; *Accepted July* 1, 2012;

Abstract The occurrence and saturation of electromagnetic (EM) instability in femtosecond laser-plasma interactions are investigated using relativistic particle-in-cell (PIC) simulations. The linear and nonlinear saturations of EM instability are discussed. It is found that for plasma of non-Maxwell velocity distribution, the initial random thermal motions of electrons induce EM instability in plasma, and the resulting intense EM field causes the deposition of energy on electron beams in a very short distance and suppresses the energy transportation of super-thermal electrons formed by the ponderomotive force of the laser. This research benefits the understanding of mechanism of self-generated magnetic fields in inertial confinement fusion (ICF).

Key words laser technique; laser-plasma interaction; electromagnetic instability; self-generated maguetic field; fast ignition

OCIS codes 140.7090; 140.3538; 320.7110

doi: 10.3788/CJL201239.s202003

1 Instroduction

Recent ultraintense laser-plasma interaction experiments have produced observations of many interesting new phenomena—such as the acceleration of electrons to energies of up to 100 MeV[1], the production of intense directional proton beams[2], and the generation of multimegagauss magnetic fields[2,3]. Such developments may one day allow construction of compact tabletop particle accelerators for applications in high-energy physics and medicine. This work has been made possibly by the implementation of chirped pulse amplification (CPA) technology in modern laser facilities, which can currently achieve focused intensities of 10^{21} W/cm^2. Under these conditions intense electron beams can be produced[4], which may be useful for igniting compressed deuterium-tritium capsules in inertial confinement fusion experiments[5]. The generation of energetic particles by the interaction of an ultraintense laser pulse with plasma has been demonstrated theoretically[1~6] and experimentally. A fast ignitor concept[5,6] is proposed to efficiently ignite the high density fusion fuel plasmas with an ultraintense short laser pulse. In the fast ignitor scheme, the intense laser pulse propagates through a colonial plasma of up to several times the critical density, and delivers energy to energetic electrons. These highly energetic particles then transport the energy through the overdense plasma to the center of the compressed core and ignite the fuel there. It is known that interactions of ultraintense laser pulses with overdense plasmas lead to the generation of a magnetic field and the so-called Weibel instability[7~14]. The Weibel-type instability breaks up the fast electron current into filaments. The magnetic fields in the linear stage are weak and do not influence the high energy electron transport. On the other hand, the magnetic fields after being nonlinearly saturated impact more on the high-energy electron flow[7~14]. The self-generated magnetic fields are stabilized by the transverse energy spread of the high-energy electron. There have been a number of reports on the Weibel instability of self-generated magnetic fields. It is very important to determine the saturated magnetic fields. A nonlinear theory is developed to lead to the saturation level of the Weibel instability.

This paper reports on the Weibel instabilities and nonlinearly saturated magnetic fields of the instabilities by using the magnetic trapping in ultraintense-laser-underdense-plasma interactions. It is found that the nonlinearly saturated magnetic fields of Weibel instabilities are determined by the laser intensity and the plasma density.

2 The mechanism of Weibel instability

If we consider a single bi-Maxwellian component of electrons with temperature anisotropy as shown in Fig. 1, perturbed magnetic fields in the z direction rotate the electron velocity distribution indicated by Figs. 1(a) and (b). Electrons which have positive region in Fig. 1(a) and have negative region in Fig. 1(b) gather together at the center point N forming a distribution like "heart" shape indicated in Fig. 1(c). Consequently an electron current is induced in the x direction at point N. Thus magnetic fields of purely growing mode are excited in the plasma.

The mechanism of spontaneous generation of prop-

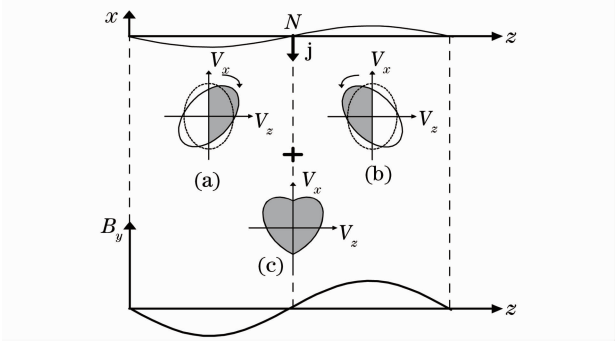

Fig. 1. Exitation mechanism of purely growing electromagnetic waves. In (a), (b) and (c), contours show isometric lines of velocity distributions.

agating electromagnetic waves can be illustrated as follows. When the electron velocity distribution has a mean drift velocity v_d along the x direction, the situation is quite same as that described above, if we look at the phenomenon in the moving frame with the velocity v_d. If we observe this in the laboratory frame, growing magnetic fields propagate with the phase velocity $\omega_r/k = v_d$, where ω_r is the real part of the angular frequency and k is the wave number.

3 Weibel-type magnetic field generation

3.1 Weibel instability

For relativistic bi-Maxwellian plasma, the growth rate of the Weibel instability takes on a maximum value[12,14]

$$f(v_x, v_y, v_z) = \frac{n}{(2\pi)^{3/2} u_x u_y u_z} \times \exp\left[-\left(\frac{v_x^2}{2u_x^2} + \frac{v_y^2}{2u_y^2} + \frac{v_z^2}{2u_z^2}\right)\right], \quad (1)$$

and also

$$\frac{1}{2} m u^2 = \frac{1}{2} k_B T, \quad (2)$$

where x-axis is the laser-irradiated one, n is the number density, v is the velocity, u is the thermal velocity, m is the mass, k_B is the Boltzmann constant, and T is the temperature.

For the bi-Maxwellian electron distribution, the maximum growth rate of the Weibel-type instability is given by[10,14]

$$\gamma^T = \sqrt{\frac{8}{27\pi}} \omega_L \sqrt{\frac{k_B T_z}{mc^2}} \frac{A^{3/2}}{A+1}, \quad (3)$$

where ω_L is laser pulse, A is an anisotropic factor and defined by

$$A \equiv \frac{T_x}{T_z} - 1, \quad (4)$$

where $T_x > T_y = T_z$.

We can calculate the growth rate of the spontaneous magnetic field in our simulation and also compare the results to our theoretical ones.

In relativistic plasmas, the trapping of the high-energy electron in the interaction region happens not only in the magnetic fields, but also in the electrostatic fields. But in relativistic bi-Maxwellian plasma, the trapping of the high-energy electron by the magnetic fields is dominant over that by the electrostatic fields.

3.2 Saturated magnetic fields

It is found that saturation occurs when the magnetic bounce frequency ω_B increases to a value comparable to the linear growth rate γ^T prior to saturation[12,14]

$$\gamma^T \cong \omega_B \equiv \sqrt{\frac{ek_z u_x B_y^T}{\gamma^2 mc}}, \quad (5)$$

where B_y^T is the saturated magnetic field in the y direction and $u_x = \sqrt{k_B T_x/m}$.

From Eqs. (3)～(5), the saturated magnetic field is given by

$$B_y^T = \frac{8\sqrt{3}}{27\pi} \sqrt{\frac{T_x}{mc^2}} \frac{A^{5/2}}{(A+1)^3} \frac{\gamma^2 m\omega_p c}{e} = \frac{8\sqrt{3}}{27\pi} [(1+\lambda_\mu^2 I_{18}/1.37)^{1/2} - 1]^{1/2} \times (1+\lambda_\mu^2 I_{18}/1.37)^{3/4} \frac{A^{5/2}}{(A+1)^3} \sqrt{\frac{n_e}{n_c}} B_0, \quad (6)$$

where $T_z = T_x/(A+1)$, $\lambda_\mu = 1.06\ \mu$m, $B_0 = m\omega_L c/e = 101$ MG and n_c is the critical density which corresponds to 9.96×10^{20} cm^{-3}. In the underdense plasmas, the high energy electron density n_{eh} is approximately set to n_e as in Eq. (6).

Furthermore, for $I_{18} \gg 1$, we find

$$B_y^T \cong 0.119 \lambda_\mu^2 \frac{A^{5/2}}{(A+1)^3} I_{18} \sqrt{\frac{n_e}{n_c}} B_0. \quad (7)$$

If we take the maximum value of $A^{5/2}/(A+1)^3$ and $\lambda_\mu = 1.06\ \mu$m, the maximum saturated magnetic field can be written as

$$B_{y,\max}^T \cong 3.48 \times 10^{-2} I_{18} \sqrt{\frac{n_e}{n_c}} B_0. \quad (8)$$

4 PIC simulation Model

We apply a PIC method to simulate the interaction of overdense plasmas with intense ultrashort laser pulses. The method is based on the electromagnetic PIC and is appropriate for the analysis of the dynamics of overdense plasma generated by arbitrarily polarized, obliquely incident laser pulse. Our PIC code is fully three-dimensional (3D) in both space (x, y, z) and velocity space (v_x, v_y, v_z) in the rectangular Cartesian coordinate system. It also takes into consideration the relativistic correction. In this code, the particle and the field quantities are derived from the time evolution of a closed differential equation set which consists of equations of electron motion and Maxwell equations, and are solved self-consistently in the given plasma systems.

Simulations are performed for a laser wavelength of 1.06 μm, laser intensity I of 10^{20} W/cm^2, and laser pulse width of 40 fs. The laser pulse is linearly polarized, normally incident, and the intensity distribution has a Gaussian shape in space. The maximum electron

density is $n_e = 5n_c$. The magnetic field associated with a intense laser $B_L = m\omega_L c/e = 101$ MG. The initial temperature of electrons and ions are 1 and 0.8 keV, respectively, and the electron-ion ratio is 1/1836. The time step is chosen to be $0.1/\omega_L$, and the spatial step is $0.3c/\omega_L$. The transverse system size is 4 μm × 4 μm, and the longitudinal length is 10 μm. The plasma has a length of 6 μm, and there are 2-μm vacuum regions on both sides of the plasma, as shown in Fig. 2. In this simulation, the coordinate x is longitudinal, and y and z are transverse. The laser polarization is in the y direction. Periodic boundary conditions are applied in the transverse direction. We assume an absorbing boundary for the fields and a thermal reflection boundary for particles in the x direction. The default numbers of spatial grids in the plasma region and particles are $200 \times 100 \times 100$ and 5×10^6, respectively.

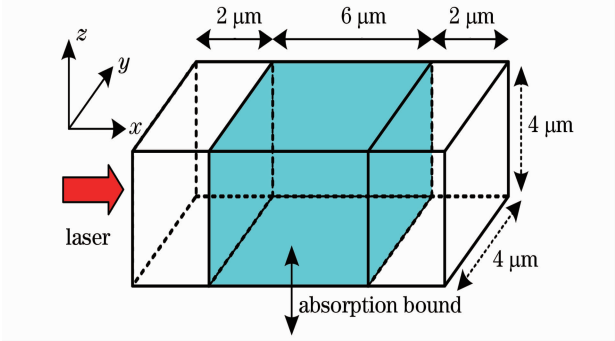

Fig. 2. Target density profile.

5 Results

In Fig. 3, the anisotropic parameter A is maximum ($A = 9.21$) at $\omega_L t = 44.1$ and $n_e = 5n_c$. From Fig. 4, we can estimate the maximum growth rate of the self-generated magnetic field at $\omega_L t = 44.1$ and the saturated magnetic field to be about $\gamma^S = 0.12\omega_L$ and $B_y^S = 0.14B_0 = 14.14$ MG, respectively, at $n_e = 5n_c$. The growth rate and the saturated magnetic field can be calculated by using Eq. (3) where u_z is shown in Fig. 5 and Eqs. (7), (8) to be about $\gamma^T = 0.15\omega_L$ and $B_y^T = 0.12B_0 = 12.12$ MG, respectively. The growth rate γ^S and the saturated magnetic field B_y^S are consistent with γ^T and B_y^T, respectively. Figure 6 shows the isosurface

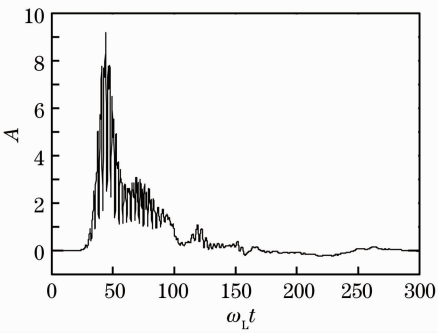

Fig. 3. Anisotropic parameter A versus $\omega_L t$ at $n_e = 5n_c$

B at $\omega_L t = 182$ (102 fs) as observed from the laser irradiation direction.

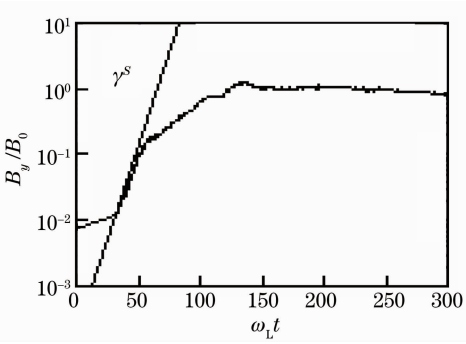

Fig. 4. Magnetic field B_y/B_0 versus $\omega_L t$ at $n_e = 5n_c$

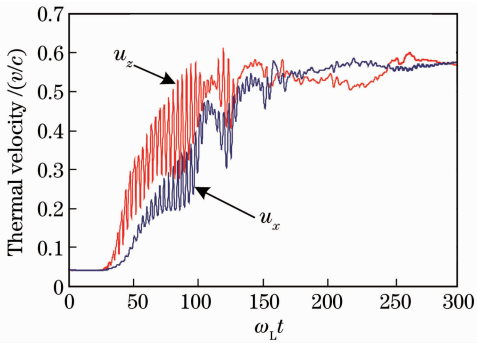

Fig. 5. Thermal velocities u_x and u_z versus $\omega_L t$

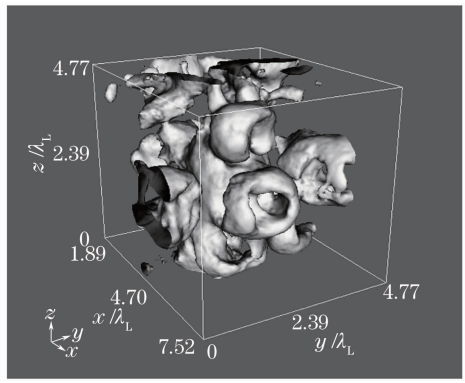

Fig. 6. 3D structure of magnetic channels at $n_e = 5n_c$ and $\omega_L t = 182$ (102 fs)

6 Conclusion

The electromagnetic instability, spatial and temporal evolution of the electron beam as propagating in collisionless plasma is studied by using the electromagnetic particle simulation. The process of the onset and nonlinear saturation of the electromagnetic instability was discussed. The dependency of the linear growth rate of the electromagnetic instability on the thermal speed of the background plasma was obtained. The theoretical and simulation results show that the values of the theoretical growth rate γ^T and the numerical simulation growth rate γ^S are fairly consistent. The anisotropy heat causes the electromagnetic instability of the laser. Due to the pondermotive force, the electrons are accelerated

in the x direction only, thereby forms the anisotropic velocity distribution ($u_x > u_z$), and stimulates the self-generated magnetic field. The simulation result also shows that when the self-generated magnetic field is excited, as the plasma density profile becomes steeper, the acceleration of the electrons in the x direction is suppressed, and the acceleration in the z direction gradually increases. Such an anisotropic distribution generated in the initial stage of the laser-plasma interaction promotes the generation of the spontaneous magnetic field. Moreover, the self-generated magnetic field in the latter moment father produces impacts on the inside of the plasma.

This work was supported by the National Natural Science Foundation of China (Nos. 10965008, 11164030).

References

1 Zheng Chunyang, Liu Zhanjun, Li Jiwei *et al*.. Spatio temporal evolution of electron beam instability in collisionless plasmas[J]. *Acta Physica Sinica*, 2005, **54**(5): 2138～2146
郑春阳，刘占军，李纪伟 等. 无碰撞等离子体中电子束流不稳定性的时空演化研究[J]. 物理学报, 2005, **54**(5): 2138～2146

2 Liu Zhanjun, Zhu Shaoping, Cao Lihua *et al*.. Study of laser plasma interactions using Vlasov and Maxwell equations [J]. *Acta Physica Sinica*, 2007, **56**(12): 7084～7089
刘占军，朱少平，曹莉华 等. 利用一维 Vlasov 和 Maxwell 方程模拟激光等离子体相互作用[J]. 物理学报, 2007, **56**(12): 7084～7089

3 Yin Yan, Chang Wenwei, Ma Yanyun *et al*.. Energetic ions generation in the interaction between ultrashort ultraintense laser pulse and solid target[J]. *High Power Laser and Particle Beams*, 2004, **16**(6): 741～744
银　燕，常文蔚，马燕云 等. 超短脉冲超强激光与固体靶相互作用中高能离子的产生[J]. 强激光与粒子束, 2004, **16**(6): 741～744

4 Cai Dafeng, Wang Lijuan, Wang Jian *et al*.. Self-generation magnetic field in the ultrashort ultrahigh laser- produced plasma research[J]. *J. Atomic and Molecular Physics*, 2009, **26**(3): 65～69
蔡达锋，王利娟，王　剑 等. 超短超强激光-等离子体中自生磁场的研究[J]. 原子与分子物理学报, 2009, **26**(3): 65～69

5 J. Fuchs, G. Malka, J. C. Adam *et al*.. Dynamics of subpicosecond relativistic laser pulse self-channeling in an underdense preformed plasma[J]. *Phys. Rev. Lett.*, 1998, **80**(8): 1658～1661

6 A. Abudurexiti, A. Zaker, P. Tuniyazi *et al*.. Effect of plasma density scale length on energetic protons generation in laser-plasma interaction [J]. *Laser and Optoelectronics Progress*, 2011, **48**(8): 083201
阿不都热苏力，艾尔肯，帕尔哈提 等. 激光等离子体密度表长对高能质子加速的影响[J]. 激光与光电子学进展, 2011, **48**(8): 083201

7 Shuai Bin, Shen Baifei, Li Ruxin *et al*.. High order harmonic generation in ultra thin plasma foil[J]. *Acta Optica Sinica*, 2002, **22**(10): 1153～1158
帅　斌，沈百飞，李儒新 等. 强激光和超薄等离子体薄膜相互作用产生高次谐波[J]. 光学学报, 2002, **22**(10): 1153～1158

8 He Minqing, Sheng Zhengming, Wu Huichun *et al*.. Effect of laser polarizations on surface instability of dense plasma irradiated by relativistic intense laser pulses[J]. *Acta Optica Sinica*, 2007, **27**(11): 2008～2012
何民卿，盛政明，武慧春 等. 离子体表面不稳定性的入射光偏振态效应[J]. 光学学报, 2007, **27**(11): 2008～2012

9 Bin Jianhui, Lei Anle, Yu Wei *et al*.. Influence of initial plasma temperature on energetic proton generation from laser-plasma interactions[J]. *Chinese J. Lasers*, 2009, **36**(6): 1416～1419
宾建辉，雷安乐，余　玮 等. 离子体初始温度对强激光与等离子体相互作用中的高能质子产生的影响[J]. 中国激光, 2009, **36**(6): 1416～1419

10 E. S. Weibel. Spontaneously growing transverse waves in a plasma due to an anisotropic velocity distribution[J]. *Phys. Rev. Lett.*, 1959, **83**(2): 83～84

11 T. Y. B. Yang, J. Arons, A. B. Langdon *et al*.. Evolution of the Weibel instability in relativistically hot electron-positron plasmas[J]. *Phys. Plasmas*, 1994, **1**(9): 3059～3078

12 K. Satou, T. Okada. Three-dimensional PIC simulation study of intense laser-irradiated targets [J]. *Fusion Engineering and Design*, 1980, **24**(3): 245～248

13 T. Okada, K. Ogawa. Saturated magnetic field for Weibel instability in ultraintense laser-plasma interactions[J]. *Phys. Plasmas*, 2007, **14**(7): 072702

14 T. Okada, T. Yabea, K. Niua. Thermal flux reduction by electromagnetic instabilities[J]. *J. Plasma Physics*, 1978, **20**(3): 405～417

栏目编辑：宋梅梅